Jpn. J. Appl. Phys. Vol. 40 (2001) pp. L 875–L 877
Part 2, No. 8B, 15 August 2001

Low-Threshold Continuous-Wave Lasing in Photopumped GaInAsP Microdisk Lasers

Masayuki FUJITA, Kousou TESHIMA and Toshihiko BABA

Faculty of Electrical and Computer Engineering, Yokohama National University, 79-5 Tokiwadai, Hodogaya-ku, Yokohama 240-8501, Japan

(Received February 19, 2001; accepted for publication June 29, 2001)

We demonstrated continuous-wave lasing at room temperature in a photopumped GaInAsP microdisk laser fabricated by Cl_2/Xe inductively coupled plasma etching. The minimum threshold pump power was as low as 30 μW. This value is 0.7 times the lowest threshold in the current injection device due to the uniform carrier distribution by photopumping. Higher thermal resistance and odd-order azimuthal mode lasing as a result of a narrower pedestal and no upper post structure were observed.

KEYWORDS: GaInAsP, microcavity, microdisk, photopumped, semiconductor laser

The microdisk laser has a sub-μm^3 order small cavity with a high Q.[1,2] Therefore, ultralow-threshold lasing by the volume effect or zero-threshold lasing by a large spontaneous emission factor C, the coupling efficiency of spontaneous emission energy to a lasing mode, close to 1[3,4] are expected. Thus, a threshold current of 40 μA[5] and a C factor of 0.1[6] were achieved in current injection devices at room temperature (RT) under a continuous-wave (cw) condition. On the other hand, photopumped devices have also been studied by many research groups.[1,7–13] They are attractive because of their simple structure, easy fabrication and evaluation, and the potential of a large-scale integration for all optical processings. However, RT cw lasing has not been achieved without special processes, *e.g.*, wafer bonding and selective oxidation.[9,13] According to discussions in refs. 9 and 13, this is due to the large thermal resistance in normal microdisks exposed to the air. However, quantitative discussion on this matter is very limited. The thermal resistance was estimated to be $0.5 - 1.5 \times 10^5$ K/W for the injection device,[14] but has never been evaluated for photopumped devices. In addition, a serious problem of the above-mentioned processes is that they degrade the active material and increase the threshold to the milliwatt order. Under such conditions, the threshold characteristic and the large C factor have not been fully investigated yet. In this study, we realized ultralow-threshold RT cw lasing in a photopumped device fabricated by the standard process we developed for the injection device. For these devices, we carefully investigated the lasing characteristic and the thermal resistance, and found some unique properties different from those of the injection device. This paper describes these results, and finally discusses the key issues for their ultimate performance.

In this experiment, we prepared an metal-organic vapor-phase-epitaxy grown 1.55-μm GaInAsP-InP wafer with a 1% compressively strained quantum-well (QW) active layer. The thickness of each of the five quaternary (Q) QWs was 5 nm, and that of 1.20-μm Q barrier layers was 12 nm. They were sandwiched by 1.20-μm Q, 1.15-μm Q and 1.10-μm Q cover layers, each of which was 30 nm thick. Cover layers were expected to suppress the carrier dissipation at disk surfaces by the surface recombination. After drawing circular dot patterns by the electron-beam lithography, vertical mesas were formed by Cl_2/Xe inductively coupled plasma etching. The key issues of this process are complete roundness, and smooth and vertical side walls. The etching condition was almost the same as that described in ref. 5 except for the Cl_2 flow rate. It was reduced to 3 sccm to suppress the appearance of crystallographic planes caused by the excess chemical reaction. The disk shape with the InP pedestal, as shown in the inset in Fig. 1, was formed by the selective wet etching of the InP lower cladding. In the measurement, the device was pumped by the 0.98-μm laser light. The emitted light was detected by a multimode fiber and analyzed by an optical spectrum analyzer. The effective pump power was estimated by the formula $P_o \cdot (a^2/w^2) \cdot (1 - R) \cdot (1 - e^{-\alpha d})$, where P_o is the irradiated power, a the disk radius, w the focused spot radius ($\sim 10\,\mu$m in this experiment), R the reflectivity at the disk surface (~ 0.3), α the average optical absorption coefficient of the disk ($\sim 2 \times 10^4$ cm^{-1}),[15] and d the disk thickness (~ 250 nm).

Figure 1 shows the laser mode peak intensity versus effective pump power characteristics at RT under the cw condition. The lowest threshold pump power P_{th} is 30 μW for the 3.0-μm-diameter device. The threshold power density is 400 W/cm^2. Using the relation $P/\hbar\omega = I/e_0$ with the angular frequency ω, the current I and the electron charge e_0, the threshold power density can be converted to a current density of 520 A/cm^2. This value is 0.7 times the lowest threshold current density for the injection device,[5] and is almost the same as that evaluated for the injection device excluding

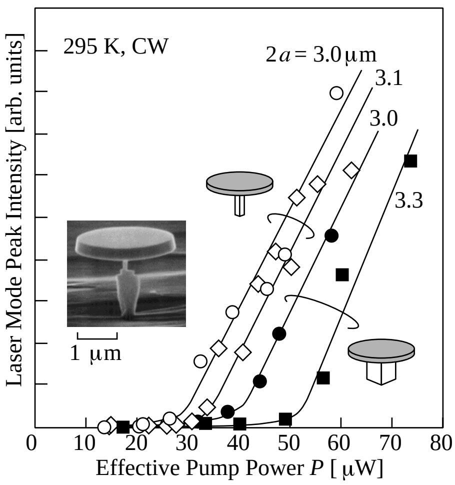

Fig. 1. Laser mode peak intensity versus effective pump power. Circles, diamonds and squares denote disk diameter $2a = 3.0$, 3.1 and 3.3 μm, respectively. Open and closed symbols represent a smaller pedestal device with a disk wing of $\sim 1\,\mu$m width exposed to air and a larger pedestal device with a disk wing of $\sim 0.5\,\mu$m width, respectively.

the excess current caused by the nonuniform carrier distribution.[5] The full width at half maximum (FWHM) of the background spontaneous emission spectrum at $1.1 \times P_{th}$ is 80 nm. This is comparable to or smaller than that observed for the injection device recording the lowest threshold current density. Considering the fact that FWHMs are generally determined by the pump level in semiconductors, the observed FWHM indicates that the estimated threshold for the photopumped device is comparable to or lower than that of the injection device. This result is consistent with the above discussion. Figure 1 also suggests that a smaller disk diameter and a smaller pedestal result in a lower threshold due to the volume effect and the reduction in light scattering loss, respectively. Regarding the scattering loss, the difference in Q factor was observed in resonant spectra at the pump level for the transparent carrier density; $Q = 3000$ for the 3.0-μm-diameter device with the smaller pedestal, while $Q = 2000$ for the 3.3-μm-diameter device with the larger pedestal.

Figure 2 shows lasing spectra of the 3.0-μm-diameter device. The lasing wavelength is 1610 nm. The mode peak intensity at $2 \times P_{th}$ is 30 dB higher than the background spontaneous emission level. The linewidth at this pump level is 0.3 nm, which is the resolution limit of the measurement. In Fig. 2, the blueshift at the lower pump level due to the carrier effect and the redshift at the higher pump level due to the thermal effect are observed, as in the injection device.[14] At the higher pump level, the observed redshift $\Delta\lambda/\Delta P$ is 20–50 nm/mW, where $\Delta\lambda$ is the wavelength shift and ΔP is the increase of the pump power. The thermal resistance is given by the expression $(\Delta\lambda/\Delta T)^{-1} \cdot (\Delta\lambda/\Delta P)$, where $(\Delta\lambda/\Delta T)$ is the temperature dependence of the wavelength shift (typically 0.1 nm/K for GaInAsP). This estimation seems to be reasonable, since the temperature increase of the InP substrate is less than 0.1 times that of the disk, even considering the free carrier absorption of the pump light in the substrate. From Fig. 2, it is estimated to be $2\text{–}5 \times 10^5$ K/W. This is higher than $0.5\text{–}1.5 \times 10^5$ K/W for injection devices having almost the same disk diameter. The reason considered is that the heat diffusion in photopumped devices with a very small pedestal is more difficult than in injection devices having a relatively large pedestal, an upper post and a contact layer.

Figure 3 shows the C factor estimated by the careful curve fitting described in ref. 6. In this experiment, spectrally integrated laser mode power versus effective pump power characteristics were obtained from far below the threshold to above threshold. Theoretical values were calculated from rate equations without the carrier diffusion effect.[2] Here, we assumed the logarithmic gain $G = G_0 \ln(N/N_0)$ with $G_0 = 150\,\text{cm}^{-1}$ and the transparent carrier density $N_0 = 1.8 \times 10^{18}\,\text{cm}^{-3}$, the radiative recombination coefficient $B = 2 \times 10^{-10}\,\text{cm}^3/\text{s}$, the Auger recombination coefficient $C_A = 5 \times 10^{-29}\,\text{cm}^3/\text{s}$ and the modal index of 2.65. The curve fitting was performed for some devices of nearly 3 μm in diameter. The small fluctuation of the diameter changed the modal wavelength and the C factor. The largest value is 0.03 for the photopumped device. However, Fig. 3 clearly shows that the experimental C factor agrees with the theoretical curve obtained by the simple expression with the observed spontaneous emission spectrum,[14] and is increased by the fine mode tuning to the spontaneous emission peak. All the lasing modes locate at longer wavelengths than the spontaneous emission peak, since the gain peak generally redshifts against the spontaneous emission peak in semiconductors. Therefore, the maximum theoretical value of 0.2 can be obtained by making the modal wavelength shorter than the gain peak.

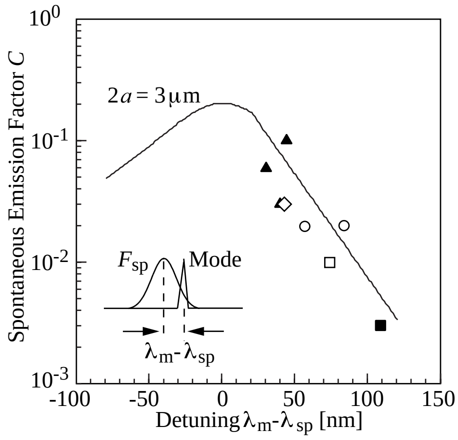

Fig. 3. Dependence of C factor on mode detuning against spontaneous emission peak. Open and closed symbols denote photopumped and current injection devices, respectively. Triangles, circles, diamonds and squares denote $2a = 2.7$, 3.0, 3.1 and 3.3 μm, respectively.

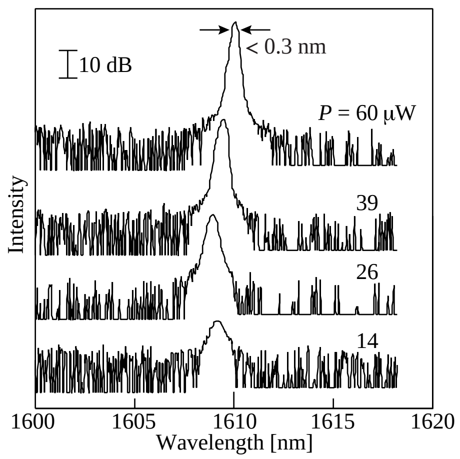

Fig. 2. Lasing spectra against various pump powers. $2a = 3.0\,\mu$m. Resolution limit of measurement is 0.3 nm.

Figure 4 shows the lasing wavelengths measured for various disk diameters. In injection devices, lasing always occurs by even-order azimuthal modes so that the scattering loss at the edge of posts having the square crosssection is minimized.[16] The finite-difference time-domain simulation of light indicates that the scattering loss at the post edge for odd-order azimuthal modes is larger than $10\,\text{cm}^{-1}$, while that for even-order azimuthal modes $\leq 2\,\text{cm}^{-1}$. However, the post width cannot be reduced freely, since it disturbs the smooth carrier diffusion. On the other hand, in uniformly photopumped devices with a sufficiently small pedestal, the scattering loss can be less than $1\,\text{cm}^{-1}$ for any modes. In fact, the 11th mode lasing is observed, as shown in Fig. 4.

In summary, we realized RT cw lasing in GaInAsP microdisk lasers by photopumping with a threshold power of 30 μW. This low value is due to the uniform excitation of the disk as well as the small disk diameter of $\sim 3\,\mu$m. The spontaneous emission factor was evaluated to be of 10^{-2} order. This

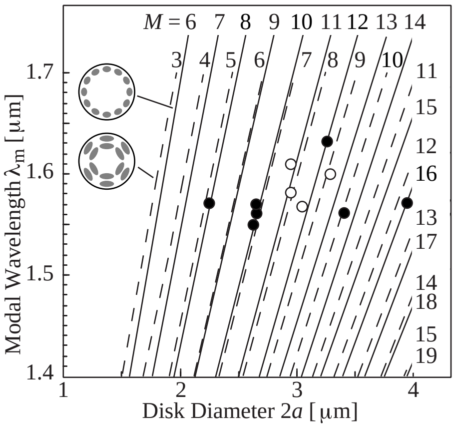

Fig. 4. Lasing wavelength versus disk diameter. Symbols and lines indicate experiment and theory, respectively. Open and closed symbols denote photopumped and current injection devices, respectively.

measurement indicated that a larger value more than 0.2 will be possible by fine mode tuning to the spontaneous emission peak. As expected, the thermal resistance was as high as the 10^5–10^6 K/W order. Thus, a low refractive index cover layer, which maintains the strong optical confinement and accelerates the heat diffusion, will be necessary for the large-scale integration of this type of device.[17] In addition, we observed the relatively weak selection of the lasing mode in this device. For stable single-mode operation, we will discuss a modified structure elsewhere.[18]

This work was partly supported by The Grant-in-Aid #13305009 by the Ministry of Education, Culture, Sports, Science and Technology, and also supported by Japan Society for Promotion of Science, Research for the Future #JSPS-RFTF 97P00103 and Research Fellowship #05045.

1) S. L. McCall, A. F. J. Levi, R. E. Slusher, S. J. Pearton and R. A. Logan: Appl. Phys. Lett. **60** (1992) 289.
2) T. Baba: IEEE J. Sel. Top. Quantum Electron. **3** (1997) 808.
3) M. K. Chin, D. Y. Chu and S. T. Ho: J. Appl. Phys. **75** (1994) 3302.
4) J. Vučković, O. Painter, Y. Xu, A. Yariv and A. Scherer: IEEE J. Quantum Electron. **35** (1999) 1168.
5) M. Fujita, R. Ushigome and T. Baba: Electron. Lett. **27** (2000) 790.
6) M. Fujita, R. Ushigome and T. Baba: IEEE Photon. Technol. Lett. **13** (2001) 403.
7) A. F. J. Levi, S. L. McCall, S. J. Pearton and R. A. Logan: Electron. Lett. **29** (1993) 1666.
8) R. E. Slusher, A. F. J. Levi, U. Mohideen, S. L. McCall, S. J. Pearton and R. A. Logan: Appl. Phys. Lett. **63** (1993) 1310.
9) S. M. K. Thiyagarajan, A. F. J. Levi, C. K. Lin, I. Kim, P. D. Dapkus and S. J. Pearton: Electron. Lett. **34** (1998) 2333.
10) B. Gayral, J. M. Gérard, A. Lemaître, C. Dupuis, L. Manin and J. L. Pelouard: Appl. Phys. Lett. **75** (1999) 1908.
11) H. Cao, J. Y. Xu, W. H. Xiang, Y. Ma, S. H. Chang, S. T. Ho and G. S. Solomon: Appl. Phys. Lett. **76** (2000) 3519.
12) P. Michker, A. Kiraz, L. Zhang, C. Becher, E. Hu and A. Imamoglu: Appl. Phys. Lett. **77** (2000) 184.
13) D. S. Song, J. K. Hwang, C. K. Kim, I. Y. Han, D. H. Jang and Y. H. Lee: IEEE Photon. Technol. Lett. **12** (2000) 954.
14) M. Fujita, A. Sakai and T. Baba: IEEE J. Sel. Top. Quantum Electron. **5** (1999) 673.
15) J. I. Pankove: *Optical Processes in Semiconductors* (Prentice-Hall, Englewood Cliffs, New Jersey, 1971) Chap. 3.
16) M. Fujita, R. Ushigome and T. Baba: *Tech. Dig. Optoelectronics & Commun. Conf., Makuhari, 2000* (Business Center for Academic Societies Japan, Tokyo, 2000) p. 546.
17) R. Ushigome, M. Fujita and T. Baba: Ext. Abstr. (48th Spring Meet. 2001); Japan Society of Applied Physics and Related Societies, 29a-ZT-10 [in Japanese].
18) M. Fujita and T. Baba: to be presented in Tech. Dig. Conf. Laser & Electro-Optics Pacific Rim, Makuhari, 2001, MA1-4.